

Infall of nearby galaxies into the Virgo cluster as traced with HST¹

Igor. D. Karachentsev

Special Astrophysical Observatory RAS, Nizhnij Arkhyz, Karachai-Cherkessian Republic,
Russia 369167

ikar@sao.ru

R. Brent Tully

Institute for Astronomy, University of Hawaii, 2680 Woodlawn Drive, Honolulu, HI 96822,
USA

Po-Feng Wu

Institute for Astronomy, University of Hawaii, 2680 Woodlawn Drive, Honolulu, HI 96822,
USA

Edward J. Shaya

Department of Astronomy, University of Maryland, College Park, MD 20742, USA

Andrew E. Dolphin

Raytheon Company, 1151 East Hermans Road, Tucson, AZ 85756, USA

Received _____; accepted _____

ABSTRACT

We measured the Tip of the Red Giant Branch distances to nine galaxies in the direction to the Virgo cluster using the Advanced Camera for Surveys on the Hubble Space Telescope. These distances put seven galaxies: GR 34, UGC 7512, NGC 4517, IC 3583, NGC 4600, VCC 2037 and KDG 215 in front of the Virgo, and two galaxies: IC 3023, KDG 177 likely inside the cluster. Distances and radial velocities of the galaxies situated between us and the Virgo core clearly exhibit the infall phenomenon toward the cluster. In the case of spherically symmetric radial infall we estimate the radius of the “zero-velocity surface” to be (7.2 ± 0.7) Mpc that yields the total mass of the Virgo cluster to be $(8.0 \pm 2.3) \times 10^{14} M_{\odot}$ in good agreement with its virial mass estimates. We conclude that the Virgo outskirts does not contain significant amounts of dark matter beyond its virial radius.

1. Introduction

In the standard Λ CDM cosmological model groups and clusters are built from the merging of already formed galaxies embedded in massive dark haloes (White & Rees, 1978). Besides the dynamically evolved core, characterized by a virial radius R_v , any cluster has a more extended region where galaxies are falling towards the cluster center. In the simplest case of spherical symmetry, the region of infall has a “surface of zero-velocity” at a radius

¹Based on observations made with the NASA/ESA Hubble Space Telescope, obtained at the Space Telescope Science Institute, which is operated by the Association of Universities for Research in Astronomy, Inc., under NASA contract NAS 5-26555. These observations are associated with program GO 12878.

R_0 which separates the cluster against the global Hubble expansion. The ratio R_0/R_v lies in the range of (3.5 – 4.0) being slightly dependent on the adopted cosmological parameter Ω_Λ (Tully, 2010, Karachentsev, 2012).

As it has been noted by different authors (Vennik 1984, Tully 1987, Crook et al. 2007, Makarov & Karachentsev 2011, Karachentsev 2012), the total virial masses of nearby groups and clusters leads to a mean local density of matter of $\Omega_m \simeq 0.08$, that is 1/3 the mean global density $\Omega_m = 0.24 \pm 0.03$ (Spergel et al. 2007). One possible explanation of the disparity between the local and global density estimates may be that the outskirts of groups and clusters contain significant amounts of dark matter beyond their virial radii, beyond what is anticipated from the integrated light of galaxies within the infall domain. If so, to get agreement between local and global values of Ω_m , the total mass of the Virgo cluster (and other clusters) must be 3 times their virial masses. A measure of this missing mass can be made by mapping the pattern of infall into the cluster (or group). Uniquely in the case of the Virgo cluster, it is possible to resolve the location of galaxies in three dimensions and separate peculiar galaxies of infall from cosmic expansion as well as from virial motions. The possibility of a massive dark superhalo around Virgo can be easily tested using accurate distances at the near surface of the Virgo infall boundary with Tip of the Red Giant Branch measurements.

As shown by Lynden-Bell (1981) and Sandage (1986), in the case of a spherical overdensity with cosmological parameter $\Lambda = 0$ the radius R_0 depends only on the total mass of a group (cluster) M_T and the age of the Universe t_0 :

$$M_T = (\pi^2/8G)R_0^3t_0^{-2}, \tag{1}$$

where G is the gravitational constant. Measuring R_0 via distances and radial velocities of galaxies outside the virial radius of the system R_v , one can determine the total mass of the

system independent of its virial mass estimate.

Numerous measurements of distances to nearby galaxies obtained recently with the Hubble Space Telescope (HST) allowed us to investigate the Hubble flow around the Local Group (Karachentsev et al. 2009) and some other nearest groups: M 81 (Karachentsev & Kashibadze, 2006), and Cen A (Karachentsev et al. 2006). The average total-to-virial mass ratio for the proximate groups, derived from R_0 via eq. (1) and from R_v , turns out to be $\langle M_T/M_v \rangle = 0.60 \pm 0.15$ (Karachentsev, 2005). But as it was noticed by Peirani & Pacheco (2006, 2008) and Karachentsev et al. (2007), in a flat universe dominated by dark energy the resulting $M_T(R_0)$ mass is higher than that derived from the canonical Lemaître-Tolman eq. (1). In the "concordant" cosmological model with Λ -term and Ω_m as a matter component eq. (1) takes a form

$$M_T = (\pi^2/8G)R_0^3H_0^2/f^2(\Omega_m), \quad (2)$$

where

$$f(\Omega_m) = (1 - \Omega_m)^{-1} - (\Omega_m/2)(1 - \Omega_m)^{-3/2} \operatorname{arccos} h[(2/\Omega_m) - 1]. \quad (3)$$

Assuming $\Omega_m = 0.24$ and $H_0 = 72 \text{ km s}^{-1} \text{ Mpc}^{-1}$, one can rewrite (2) as

$$(M_T/M_\odot) = 2.12 \times 10^{12} (R_0/\text{Mpc})^3. \quad (4)$$

It yields a mass that is 1.5 as large as derived from the classic eq. (1). This correction leads to a good agreement on average between the R_0 mass estimates and virial masses for the above mentioned galaxy groups.

The most suitable object to explore the infall phenomena on a cluster scale is the

nearest massive cluster of galaxies in Virgo. The kinematics and dynamics of Virgo cluster infall were studied by Hoffman et al. (1980), Tonry & Davis (1981), Hoffman & Salpeter (1982), Tully & Shaya (1984), Teerikorpi et al. (1992), and Ekholm et al. (1999, 2000). In a model developed by Tonry et al. (2000, 2001) based on distance measurements of 300 E and S0 galaxies via their surface brightness fluctuations, the Virgo cluster with its center distance 17 Mpc and virial mass $M_v = 7 \times 10^{14} M_\odot$ generates an infall velocity of the Local Group (LG) towards Virgo of about 140 km s^{-1} . With this value of the virial mass, the expected radius of the infall zone is $R_0 = 7.0 \text{ Mpc}$ or $\Theta_0 = 23^\circ$ in angular measure. Recently, Karachentsev & Nasonova (2010) considered the existing data on radial velocities and distances of 454 galaxies situated within $\Theta = 30^\circ$ around the Virgo and came to the conclusion that the value of the radius R_0 lies in the range $[5.0 - 7.5] \text{ Mpc}$. In the standard Λ CDM model with the parameters $\Omega_m = 0.24$ and $H_0 = 72 \text{ km s}^{-1} \text{ Mpc}^{-1}$ (Spergel et al. 2007), these quantities of R_0 correspond to a total cluster mass $M_T = [2.7 - 8.9] \times 10^{14} M_\odot$. The mass estimate derived from external galaxy motions does not contradict the virial mass obtained from internal motions. However, the present accuracy is insufficient to judge whether or not the periphery of the Virgo cluster contains a significant amount of dark matter outside its virial radius $R_v = 1.8 \text{ Mpc}$ (Hoffmann et al. 1980).

2. Expected pattern of the infall

Fig. 1 represents the picture of Virgocentric infall based on current observables collected by Karachentsev & Nasonova (2010). It shows a relation between radial velocities in the LG rest frame and distances of galaxies within a cone of radius $\Theta_v = 6^\circ$, covering the virialized core. Galaxy samples with distances derived by different methods are marked by different symbols. The unperturbed Hubble flow with a slope of $H_0 = 72 \text{ km s}^{-1} \text{ Mpc}^{-1}$ is given by an inclined dashed line. The solid and dotted lines correspond to the mean Hubble

flow in a model of a point-like cluster mass with 2.7×10^{14} and $8.9 \times 10^{14} M_{\odot}$.

The distance of the Virgo cluster itself is now well established by observations of Cepheid variables in 4 galaxies. The Cepheid distances anchor precision *relative* distances for 84 galaxies with HST SBF measurements (Mei et al. 2007, Blakeslee et al. 2009) and 4 galaxies with SNIa measurements (Jha et al. 2007). These galaxies reside in the cluster core at $R_{LG} = (16.5 \pm 2)$ Mpc and therefore are useless as tracers of the Virgocentric infall.

At large distances on the diagram, behind the Virgo cluster, while most distance measures are based on the optical or IR Tully-Fisher relation with typical errors of $\sim 20\%$, there is one very well constrained group. The Virgo W' group around NGC4365 (de Vaucouleurs 1961) with $\langle V_{LG} \rangle \simeq 1000 \text{ km s}^{-1}$ contains one galaxy with both a Cepheid and SNIa measurement and 5 other galaxies with HST SBF measurements. These observations locate Virgo W' at 23 Mpc, 6.5 Mpc behind Virgo. The group velocity and distance indicate that this group lies very near the edge of the Virgo infall zone at R_0 on the far side of the cluster.

The most feasible way to trace the Z-like wave of Virgocentric infall in detail is to make distance measurements to galaxies on the *front* side of the cluster via TRGB. This method (Lee et al. 1993) is applicable to galaxies of all morphological types and provides the needed distance accuracy of $\sim 5\text{--}7\%$ (Rizzi et al. 2007). The greatest precision will be achieved with lines-of-sight tight to the cluster where projection factors with radial motions will be minimal. Unfortunately, in the virial cone $\Theta_v = 6^\circ$, there is no foreground galaxy with a literature TRGB distance. In the wider area with $\Theta < 15^\circ$ there are only 2 galaxies: NGC 4826 and GR-8 with existing TRGB distances between the LG and Virgo.

3. Selection of targets

The scarcity of TRGB data on the near side of the Virgocentric infall wave can be understood. In the past, targets for TRGB distance measurements with HST were usually galaxies from the Kraan-Korteweg & Tammann (1979) sample with radial velocities $V_{LG} < 500 \text{ km s}^{-1}$. In the Virgo core direction a galaxy with a velocity $\sim 500 \text{ km s}^{-1}$ may be a representative of the Local Volume ($R_{LG} < 10 \text{ Mpc}$), or a Virgo cluster member, or even be situated behind the cluster at $R_{LG} \simeq 20 \text{ Mpc}$ and infalling toward us. The selection of candidates that might be true nearby galaxies hidden among the huge number of Virgo cluster members is a complicated task. That is why Kraan-Korteweg & Tammann (1979) even excluded the Virgo cluster core ($\Theta < 6^\circ$) from their consideration.

The expected number of missed nearby galaxies in the region $RA = [12.0^h - 13.0^h]$, and $Dec = [0^\circ - 25^\circ]$ can be estimated as follows. The Catalog of Neighboring Galaxies (Karachentsev et al. 2004) contains 450 objects with $R_{LG} < 10 \text{ Mpc}$ distributed over the entire sky. In a new version of the catalog by Karachentsev et al. 2013 (=UNGC), updated with fresh data from recent optical and HI surveys (SDSS, HIPASS, ALFALFA, etc.) there are about 800 candidates in almost the same volume to a radius of 11 Mpc. Assuming that UNGC sample is $\sim 100\%$ complete to $M_B = -12 \text{ mag}$ and taking into account the inhomogeneous distribution of galaxies due to the concentration towards the Supergalactic equator as well as the presence of the Zone of Avoidance along the Milky Way, one can estimate the expected number of nearby ($R_{LG} < 11$) galaxies within the identified $15^\circ \times 25^\circ$ square as $\simeq 40$.

We undertook a special search for likely foreground galaxies, inspecting SDSS images of more than 2000 objects in the specified area. Among these we found 37 galaxies with HI line widths that yield Tully-Fisher distances less than $\sim 11 \text{ Mpc}$. Their radial velocities lie in the range $V_{LG} = (400 - 1400) \text{ km s}^{-1}$, and the majority of these turn out to be blue

dwarf galaxies showing no apparent concentration towards the Virgo center. As objects for our pilot program to measure distances with ACS HST via TRGB, we selected 8 galaxies which have lower Tully-Fisher distance estimates. In the target list we also included the S0-type galaxy NGC 4600 with a distance estimate via surface brightness fluctuations by Tonry et al. (2001). (The case of the nearby S0a galaxy NGC 4826 with $D(\text{sbf}) = 7.48$ Mpc (Tonry et al. 2001) and $D(\text{trgb}) = 4.37$ Mpc (Jacobs et al. 2009) tells us that these methods sometimes give distance estimates with a significant difference. At present all nine our targets have been imaged with HST within GO 12878.

Galaxies situated on the nearby boundary of the “zero velocity sphere” will have radial velocities close to the mean cluster value, $\langle V_{\text{Virgo}} \rangle = 1000 \text{ km s}^{-1}$ and, given the expected value $R_0 \simeq 7$ Mpc, distances $R_{LG} \simeq 10$ Mpc. The F814W and F606W images of these galaxies obtained with ACS at HST in a two orbit per object mode can determine their TRGB distances with an accuracy of $\sim 7\%$ or ~ 0.7 Mpc. Given a total mass of the cluster within the radius R_0 expresses by eq.(4), then the measurement of $R_0 \simeq 7$ Mpc with an accuracy of ~ 0.7 Mpc can yield a mass of the Virgo cluster with an error of $\sim 30\%$.

4. Observations and data processing

We have observed 9 galaxies with the Advanced Camera for Surveys (ACS) during the HST Cycle 20 (proposal 12878). Between November 15, 2012 and March 30, 2013 we obtained 2080s F606W and 1640s F814W images of each galaxy using ACS/WFC with exposures split to eliminate cosmic ray contamination. The images were obtained from the STScI archive, having been processed according to the standard ACS pipeline. Stellar photometry was obtained using the ACS module of DOLPHOT (<http://americano.dolphinim.com/dolphot>), the successor to HSTPHOT (Dolphin 2000), using the recommended recipe and parameters. In brief, this involves the following steps.

First, pixels that are flagged as bad or saturated in the data quality images were marked in the data images. Second, pixel area maps were applied to restore the correct count rates. Finally, the photometry was run. In order to be reported, a star had to be recovered with S/N of at least five in both filters, be relatively clean of bad pixels (such that the DOLPHOT flags are zero) in both filters, and pass our goodness of fit criteria ($\chi \leq 2.5$ and $|sharp| \leq 0.3$). These restrictions reject non-stellar and blended objects. At the high Galactic latitude of the Virgo cluster foreground stars from the Milky Way are insignificant contaminants. For some of the most distant galaxies we extended to stars with $S/N > 2$ in order to evaluate the TRGB. This extension introduces a lot of noise which is monitored by plotting CMD of empty regions beside the galaxy body.

The TRGB is determined by a maximum likelihood analysis monitored by recovery of artificial stars (Makarov et al. 2006). Artificial stars with a wide range of known magnitudes and colors are imposed at intervals over the surface of the target and recovered (or not) with the standard analysis procedures to determine both photometric errors and completeness in the crowded field environments. The maximum likelihood procedure considers the luminosity function of stars with colors consistent with the red giant branch after compensating for completeness and assesses power law fits to the distributions above and below a break identified with the TRGB. The slope of the power law faintward of the TRGB break is expected to be approximately 0.3 on a magnitude scale after correction for completeness. If the RGB is sufficiently observed to well below the tip then the slope can be a free parameter within a restricted range but in the current cases with distances approaching the effective observational limits the slope of the luminosity function fit below the TRGB is set to the expected value of 0.3. Galactic extinction, minor at the polar location of the Virgo cluster, is taken from Schlafly & Finkbeiner (2011).

The greatest potential for serious error with a TRGB measurement comes about with

confusion of the asymptotic giant branch (AGB) for the RGB. Stars on the AGB that are burning both helium and hydrogen in shells closely parallel and overlap the RGB on a CMD but rise as much as a magnitude brighter. Their peak brightness, dependent on age and metallicity, can be misinterpreted as the TRGB. AGB stars have intermediate ages of 1-10 Gyr although they are only in sufficient quantity to be confusing at the lower end of that age range (Jacobs et al. 2011). A general strategy that we employ is clipping of the area of the HST image to avoid regions of young and intermediate age stars (and regions beyond the target dominated by background and foreground contaminants) in order to maximize the contrast of the old population contributing to the RGB.

The calibration of the absolute value of the TRGB including a small color term has been described by Rizzi et al. (2007). The RGB is redder for older or more metal rich populations but galaxies inevitably have old and metal poor components, resulting in reasonable stability of tip magnitudes in the F814W band. Images, color-magnitude diagrams, photometry tables, TRGB measurements, and distance determinations are made available at <http://edd.ifa.hawaii.edu> by selecting the catalog CMDs/TRGB (Jacobs et al 2009).

5. TRGB distances to nine target galaxies

Images of our target galaxies taken from Sloan Digital Sky Survey (<http://www.sdss.org/>) are shown in Figure 2. Each field has a size of 6 by 6 arcminutes. North is up and East is left. The ACS HST footprints are superimposed on the SDSS frames. In Figure 3 a mosaic of enlarged ACS (F606W + F814W) images of the nine galaxies are shown. Their size is 1 arcminute, North is up and East is left. Color magnitude diagrams (CMDs) of F814W versus (F606W - F814W) are presented in Figure 4.

A summary of some basic parameters for the observed galaxies as well as the resulting distance moduli for them are given in Table 1. Some additional comments about the galaxy properties are briefly discussed below.

Table 1: Target galaxies in front of the Virgo cluster observed with HST.

Name	RA (J2000) Dec	V_{LG}	D	Θ	B_T	T	m_{FUV}	m_{21}	W_{50}	I_{TRGB}	D_{HST}
(1)	(2)	(3)	(4)	(5)	(6)	(7)	(8)	(9)	(10)	(11)	(12)
IC3023	121001.7+142201	710	7.7 tf	5.4	15.35	10	16.78	16.33	44	~ 27	~ 17
GR34	122207.6+154757	1205	8.9 tf	4.0	15.95	10	19.04	18.24	25	$25.94^{+0.28}_{-0.15}$	9.29 ± 0.93
U7512	122541.3+020932	1354	10.6 tf	10.3	15.20	10	17.40	15.31	65	$26.37^{+0.08}_{-0.09}$	11.8 ± 1.2
N4517	123245.5+000654	978	9.7 tf	12.3	11.09	7	15.86	12.39	307	$25.67^{+0.16}_{-0.12}$	8.34 ± 0.83
IC3583	123643.5+131534	1024	7.6 tf	1.7	13.31	9	15.43	15.66	105	$26.04^{+0.06}_{-0.05}$	9.52 ± 0.95
KDG177	123958.5+134653	913	8.2 tf	2.6	16.36	10	18.47	16.17	30	~ 27	~ 17
N4600	124023.0+030704	713	7.4 sb	9.6	13.70	0	20.38	—	—	$25.78^{+0.05}_{-0.05}$	8.90 ± 0.89
VCC2037	124615.3+101212	1038	7.4 tf	3.3	15.80	10	17.90	18.50	29	$26.01^{+0.22}_{-0.17}$	9.63 ± 0.96
KDG215	125540.5+191233	362	5.5 tf	9.1	16.90	10	18.86	15.79	25	$24.33^{+0.07}_{-0.06}$	4.83 ± 0.34

(1) galaxy name, (2) equatorial coordinates, (3) radial velocity in km s^{-1} in the LG rest frame from NASA Extragalactic Database (<http://ned.ipac.caltech.edu/>), (4) linear distance (in Mpc) as given in UNGC, estimated via Tully-Fisher relation (tf) or from surface brightness fluctuations (sb), (5) angular separation Θ (in degrees) from the Virgo cluster center that has been identified with NGC4486, (6) apparent integrated B- magnitude as given in UNGC, (7) morphological type in de Vaucouleurs scale, (8) far-ultraviolet integrated magnitude from the Galaxy Evolution Explorer (GALEX) space telescope (Gil de Paz et al. 2007), (9) HI-line magnitude $m_{21} = 17.4 - 2.5 \log F_{HI}$, where F_{HI} is an HI-flux in Jy km/s from Haynes et al (2011) or the Lyon Extragalactic Database =LEDA (<http://leda.univ-lyon1.fr/>), (10) HI-line width (in km/s) at the 50% level of the maximum, (11) TRGB magnitude and its 68% uncertainty from the maximum likelihood analysis. (12) the linear distance (in Mpc) and conservative global characterization of 10% uncertainty for

a one-orbit ACS observation of a galaxy near 10 Mpc.

GR34=VCC530, UGC7512 and VCC2037. These are irregular type dwarf galaxies with narrow HI lines. New TRGB distances to them agree with the Tully-Fisher distances confirming all the galaxies to be situated in front of Virgo cluster.

NGC4517. This Sd galaxy seen edge-on has the major angular diameter about 12', extending far beyond the ACS frame. Its CMD is constructed from an outskirts field along the minor axis to sample the halo and avoid crowded dusty regions of star formation. The TF distance to NGC 4517 is consistent with the TRGB distance.

IC3583. This Magellanic type dwarf has an asymmetric diffuse halo extended to the West. The field contributing to the CMD that is shown in Fig. 4 is clipped to minimize young and intermediate age populations and optimize the contribution of the old population. See Figure 5 for the CMD for the full ACS field and an outline of the excised region containing many young stars. Together with a bright spiral galaxy NGC 4569, IC3583 forms the optical pair Arp 76 having a radial velocity difference of 1245 km/s. The NW part of NGC 4569 is seen in the SE corner of the ACS frame. Our estimate of distance to NGC 4569 via its TRGB yields $D > 17$ Mpc.

NGC4600. This is a gas-poor dwarf lenticular galaxy with $H\alpha$ emission in the core (Karachentsev & Kaisin, 2010). We recognize a moderate agreement in the distance estimates for NGC 4600 via surface brightness fluctuations (Tonry et al. 2001) and from TRGB. It is a bit unexpected to find this isolated dS0 galaxy in front of the Virgo cluster rather than in the virial core.

KDG215=LEDA44055. This galaxy is gas-rich low surface brightness dwarf with a narrow HI-line, a high hydrogen mass-to-stellar mass ratio $M_{HI}/M_* = 3.1$, and a narrow RGB characteristic of a low metallicity system. KDG215 lies more than a magnitude closer

than any of the other targets, at 4.8 Mpc.

IC3023 and KDG177=VCC1816. Both the galaxies of Im- type are HI-rich and active star formation objects typical of field galaxies. In spite of their narrow HI-lines: 44 and 30 km/s, they both appear to belong to the Virgo cluster. The TRGB are not seen as would have been the case if these galaxies were in the Virgo foreground. In each case, the TRGB is probably being seen around $I \sim 27$ as expected for a cluster member. These tentative measurements are at the limit of the current HST photometry and we do not attempt a distance determination.

Apart from these objects, there are five other galaxies in front of the Virgo cluster that have accurate distance measurements. Information about them is collected in Table 2. We use the data on distances and radial velocities of these 7 + 5 galaxies from Tables 1 and 2 to trace the near-side Virgocentric infall. Two probable Virgo core galaxies with uncertain distances: IC 3023 and KDG 177 are excluded from consideration. In addition, the analysis will include the galaxy NGC 4365 in the Virgo W' cloud as a representative with an accurate distance of the back-side infall to the Virgo cluster. Its parameters are given in the last line of Table 2.

6. Estimating the total mass of the Virgo cluster

As noted above, the analysis of available observational data on radial velocities and distances for several hundred galaxies in the vicinity of the Virgo cluster lead to the conclusion that the radius of the zero velocity surface of the cluster lies in the range $R_0 = (5.0 - 7.5)$ Mpc (Karachentsev & Nasonova, 2010). According to equation (4) this scatter in R_0 leads to a wide scatter in the total mass estimates of the cluster, $M_T = (2.7 - 8.9) \times 10^{14} M_\odot$, exceeding a factor of three. New accurate distance measurements

Table 2: Other galaxies in front or back of the Virgo cluster with accurate distance measurements

Name	RA (J2000)	Dec	V_{LG}	D	Θ	B_T	T	Reference
N4527	123408.4+023913		1591	14.1±1.4	SN	9.8	11.38	4 Jha et al. 2007
N4536	123427.0+021117		1662	14.3±1.4	cep	10.3	11.16	4 Riess et al. 2005
N4725	125026.6+253003		1176	12.4±1.2	cep	13.9	10.11	2 Freedman et al. 2001
N4826	125644.2+214105		365	4.37±0.44	TRGB	11.2	9.30	2 Jacobs et al. 2009
GR-8	125840.4+141303		139	2.13±0.21	TRGB	9.1	14.79	10 Tully et al. 2006
N4365	122428.3+071904		1112	23.1±2.3	sbf	5.3	10.52	-3 Blakeslee et al. 2009

The column designations are similar to those in Table 1.

to relatively few galaxies residing near the front side of Virgo fix the R_0 and M_T quantities in a narrower interval.

Figure 6 reproduces a pattern of the Hubble flow in front and back of the Virgo cluster restricted to the most accurate constraints. Compared with Figure 1, it exhibits a much more distinct character of the infall. Open circles in the Fig. 6 show the galaxies from Table 2 with accurate distance estimates. The solid circles correspond to seven galaxies in front of the Virgo cluster with distances measured in this program with HST. The horizontal bars indicate distance errors. The grey vertical column denotes the zone of virial motions corresponding to the mean distance to the cluster $\langle D \rangle = 16.5 \pm 0.4$ Mpc (Mei et al. 2007) and the virial radius $R_v = 1.8$ Mpc. The inclined dashed line indicates the unperturbed Hubble flow with the parameter $H_0 = 72$ km/s/Mpc.

The average angular separation of the 12 galaxies situated in front of Virgo from its center is $\langle \Theta_v \rangle = 8.7^\circ$. The solid wave-like line in the figure reproduces the behaviour of Hubble flow perturbed by a point-like mass $M_T = 8.0 \times 10^{14} M_\odot$ at the average angular separation 8.7° from the Virgo center.

To determine the radius R_0 , one needs to fix the mean radial velocity of the cluster, $\langle V_{Virgo} \rangle_{LG}$ in the rest frame of the Local Group. According to Binggeli et al. (1993), it equals to $+946 \pm 35$ km/s. This estimate was obtained over a large number of galaxies with measured velocities but unmeasured distances, whose membership in the Virgo cluster was considered to be probable. Basing on the galaxies with membership in Virgo confirmed by accurate distances, Mei et al. (2007) derived the mean cluster velocity of $+1004 \pm 70$ km/s. The difference of 58 km/s between these estimates can be caused by a specific selection affecting Binggeli’s estimate. In a spherical layer between the radii R_v and R_0 bounded by a cone with the angular radius of $\Theta_0 \sim 20^\circ$, the expected number of galaxies behind the cluster is greater than that in front of the cluster. In the case of radially infalling galaxies into the cluster core, the difference in galaxy number falling toward us and away from us should artificially decrease the mean radial velocity of the sample. Probably, any (unknown) pre-selection effect on velocities could also be in the list of targets investigated by Mei et al. (2007). We adopt the average of these two independent values as the radial velocity of the Virgo cluster centroid, $\langle V_{Virgo} \rangle_{LG} = 975 \pm 29$ km/s, shown in Figure 6 as the horizontal dashed line.

As seen from Fig. 6, the straight line of unperturbed Hubble flow with the parameter $H_0 = 72$ km/s/Mpc crosses the Virgo center at $V_{LG} = +1188$ km/s which corresponds to the infall velocity of LG toward the Virgo: $\Delta V_{LG} = (975 \pm 29) - 72(16.5 \pm 0.4) = -213 \pm 41$ km/s. This quantity is not significantly higher than the previous estimates -139 km/s (Tonry et al. 2001) and -185 km/s (Tully et al. 2008).

The presented data exhibit also that the solid wave-like line crosses the line of the mean cluster velocity at the distance of 9.3 Mpc. Therefore, the radius of the zero-velocity surface around the Virgo cluster turns out to be $R_0 = 16.5 - 9.3 = 7.2$ Mpc. There are at least three circumstances affecting this estimate: a) uncertainty of the Virgo center

position, which is ~ 0.4 Mpc, b) uncertainty of the mean velocity of the cluster ~ 30 km/s corresponding to ~ 0.3 Mpc on the distance scale, and c) the mean-square scatter of galaxies with respect to the Z-like line that consists of ~ 0.5 Mpc. Considering these factors as being statistically independent, we obtain the sought-for radius

$$R_0 = (7.2 \pm 0.7)\text{Mpc}.$$

According to equation (4), this quantity corresponds to the total mass of the Virgo cluster

$$M_T = (8.0 \pm 2.3) \times 10^{14} M_\odot.$$

Virial mass estimates for the Virgo are: 6.2 (de Vaucouleurs, 1960), 7.5 (Tully & Shaya, 1984) and 7.2 (Giraud, 1999) in units of $10^{14} M_\odot$. These values all have been normalized to the Virgo cluster distance of 16.5 Mpc. As one can see, the total cluster mass estimate via R_0 is consistent with the average virial mass estimate, $M_v = (7.0 \pm 0.4) \times 10^{14} M_\odot$. Consequently, the zone of infall, at a radius 4 times the virial radius (assuming $\Omega_m = 0.24$), does not contain a large amount of mass outside R_v . This conclusion agrees with the results of N-body simulations performed by Rines & Diaferio (2006) and Anderhalden & Diemand (2011) for a cluster dark matter profile. These authors obtained the M_T/M_v ratio to be 1.19 and 1.25, respectively.

We draw attention to the regularity of the infall pattern seen in front of the Virgo cluster. A scatter of 12 galaxies along the vertical scale with respect to the Z-shape line under parameters $M_T = 8.0 \times 10^{14} M_\odot$ and $\langle \Theta \rangle = 8.7^\circ$ corresponds to $\sigma_v = 155$ km/s. When the difference of the individual Θ of the galaxies is taken into account, the value of

σ_v drops to 130 km/s. An essential part of this scatter, ~ 90 km/s, is caused by errors of the distance measurements, which are $\sim (7 - 10)\%$. After a quadratic subtraction of the component related to distance errors, the remaining (“cosmic”) dispersion of radial velocities turns out to be ~ 95 km/s. Therefore, one can say that the infall flow pattern around the Virgo cluster looks to be rather “cold”.

7. Concluding remarks.

The measurements of distances to nearby galaxies with the Hubble Space Telescope makes the picture of galaxy infall into the Virgo cluster much more distinct. Among nine galaxies selected as Virgo foreground candidates for our pilot HST GO 12878 program, seven reside in the expected near region while two others are probably cluster members. In our list of targets for HST there are ~ 30 more galaxies with Tully-Fisher distances around 10 Mpc. Measurements of their distances with ACS HST can give us a more precise estimate of the total mass of the nearest large cluster via infalling galaxy motions. Multicolor images of galaxies that have been obtained with the 3.5-meter CFHT telescope under the program “Next Generation Virgo Cluster Survey” (Ferrarese et al. 2012) will be useful in choosing the best candidates for new HST observations.

In the framework of the simplest spherically-symmetric radial infall of galaxies into a point-like central mass, the observed distances and radial velocities of galaxies in front of Virgo yield the value of total mass of the cluster in good agreement with the virial mass: $M_T = (1.14 \pm 0.35)M_v$. It should be stressed here that the quantity $M_T = (8.0 \pm 2.3) \times 10^{14}M_\odot$ was obtained in the case of standard Λ CDM model with the parameter $\Omega_\Lambda = 0.76$. In the old cosmological model with $\Omega_\Lambda = 0$, the estimate of total mass of the Virgo cluster via motions of surrounding galaxies would be (35–40)% lower, pushing mass estimates almost out of the confidence interval below virial mass estimates

derived via internal motions. This circumstance can be considered as another display of the existence of dark energy on a local scale of ~ 10 Mpc. It can be noted that Tully & Shaya (1984) had already used a similar argument to suggest that a Λ - term might be appropriate to explain the total kinematic pattern of the Virgo cluster.

According to our estimate, the Hubble flow around the Virgo cluster looks to be rather cold with a characteristic line-of-sight scatter ~ 95 km/s. This preliminary result, if confirmed, may impose constraints on some models of cluster formation. More new accurate distance measurements with HST are required to check this claim.

As was noted by Karachentsev et al. (2003) and Tully et al. (2008, 2013), the nearby galaxies residing inside a radius of ~ 6 Mpc around the Local Group form a flat configuration (the “Local Sheet”) with surprisingly low peculiar velocities of the barycenters of groups of ~ 30 km/s. A hint to the existence of the Local Sheet can be seen in Figure 6 too, where three the nearest galaxies: GR-8, NGC 4826, and KDG 215 all within $D = 5$ Mpc, follow remarkably well the unperturbed Hubble flow. To our knowledge, the existence of such calm domain structures, like the Local Sheet, still has not sufficiently attracted the attention of cosmologists.

Acknowledgements. The authors thank anonymous referee for thorough examination of the manuscript and for useful comments and suggestions to improve the text. Support for the program GO 12878 was provided by NASA through a grant from the Space Telescope Science Institute, which is operated by the Association of Universities for Research in Astronomy, Inc., under NASA contract NAS 5-26555. I.K. acknowledges support by RFBR-DST grant 13-02-92690 and RFBR-DFG grant 12-02-91338.

References.

- Anderhalden D., Diemand J., 2011, MNRAS, 414, 3166
- Binggeli B., Popescu C.C., Tammann G.A., 1993, A&A, 98, 275
- Blakeslee, J.P., Jordan, A., Mei, S., et al. 2009, ApJ, 694, 556
- Crook A.C., Huchra J.P., Martimbeau N. et al., 2007, ApJ, 655, 790
- de Vaucouleurs, G. 1961, ApJS, 6, 213
- de Vaucouleurs, G. 1960, ApJ, 131, 585
- Dolphin, A. 2000, PASP, 112, 1383
- Ekholm T., Lanoix P., Teerikorpi P., Fouque P., Paturel G., 2000, A&A, 355,835
- Ekholm T., Lanoix P., Teerikorpi P., Paturel G., Fouque P., 1999, A&A, 351, 827
- Ferrarese L., Cote P., Cuillandre J. et al. 2012, ApJS, 200, 4
- Freedmann W.L., Madore B.F., Gibson B.K. et al. 2001, ApJ, 553, 47
- Gil de Paz A., Boissier S., Madore B.F., et al. 2007, ApJS, 173, 185
- Giraud E., 1999, ApJ, 524, L15
- Haynes M.P., Giovanelli R., Martin A.M., et al. 2011, AJ, 142, 170
- Hoffman G.L., Salpeter E.E., 1982, ApJ, 263, 485
- Hoffman G.L., Olson D.W., Salpeter E.E., 1980, ApJ, 242, 861
- Jha, S, Riess, A.G., Kirshner, R.P. 2007, ApJ, 659, 122
- Jacobs, B.A., Rizzi, L, Tully, R.B. et al. 2009, AJ, 138, 332
- Jacobs, B.A., Tully, R.B., Rizzi, L., et al. 2011, AJ, 141, 106

- Karachentsev I.D., Makarov D.I., Kaisina E.I., 2013, AJ, 145, 101 (UNGC)
- Karachentsev I.D., 2012, Ast.Bull. 67, 115
- Karachentsev I.D., Nasonova O.G., 2010, MNRAS, 405, 1075
- Karachentsev I.D., Kaisin S.S., 2010, AJ, 140, 1241
- Karachentsev I.D., 2005, AJ, 129, 178
- Karachentsev I.D., Karachentseva V.E., Huchtmeier W.K., Makarov D.I., 2004, AJ, 127, 2031 (CNG)
- Karachentsev I.D., Makarov D.I., Sharina M.E., et al. 2003, A&A, 398, 479
- Kraan-Korteweg R.C., Tammann G.A., 1979, Astron. Nachr., 300, 181
- Lee M.G., Freedman W.L., Madore B.F., 1993, AJ, 106, 964
- Lynden-Bell D., 1981, The Observatory, 101, 111
- Makarov D.I., Karachentsev I.D., 2011, MNRAS, 412, 2498
- Makarov, D.I, Makarova, L., Rizzi, L. et al. 2006, AJ, 132, 2729
- Mei S., Blakeslee J.P., Côté P., Tonry J.L., et al., 2007, ApJ, 655, 144
- Peirani S, Pacheco J.A., 2008, A & A, 488, 845
- Peirani S, Pacheco J.A., 2006, New Astr., 11, 325
- Riess A.G., Li W., Stetson P.B., et al. 2005, ApJ, 627, 579
- Rines K., Diaferio A., 2006, AJ, 132, 1275
- Rizzi L., Tully R.B., Makarov D.I., et al., 2007, ApJ, 661, 813
- Sandage A., 1986, ApJ, 307, 1

- Schlaflly, E.F., Finkbeiner, D.P., 2011, ApJ, 737, 103
- Spergel D.N., et al., 2007, ApJS, 170, 377
- Teerikorpi P., Bottinelli L., Gouguenheim L., Paturel G., 1992, A&A, 260, 17
- Tonry J.L., Schmidt B.P., Barris B., et al., 2003, ApJ, 594, 1
- Tonry J.L., Dressler A., Blakeslee J.P., et al., 2001, ApJ, 546, 681
- Tonry J.L., Davis M., 1981, ApJ, 246, 680
- Tully R.B., Courtois H.M., Dolphin A.E., et al. 2013, AJ, 146, 86
- Tully R.B., Shaya E.J., Karachentsev I.D., et al., 2008, ApJ, 676, 184
- Tully R.B., Rizzi L., Dolphin A.E., et al., 2006, AJ, 132, 729
- Tully R.B., 1987, ApJ, 321, 280
- Tully R.B., Shaya E.J., 1984, ApJ, 281, 31
- Tully R.B., 2010, arXiv:1010.3787
- Vennik J., 1984, Tartu Astron. Obs. Publ., 73, 1
- White S.D.M., Rees M.J., 1978, MNRAS, 183, 341

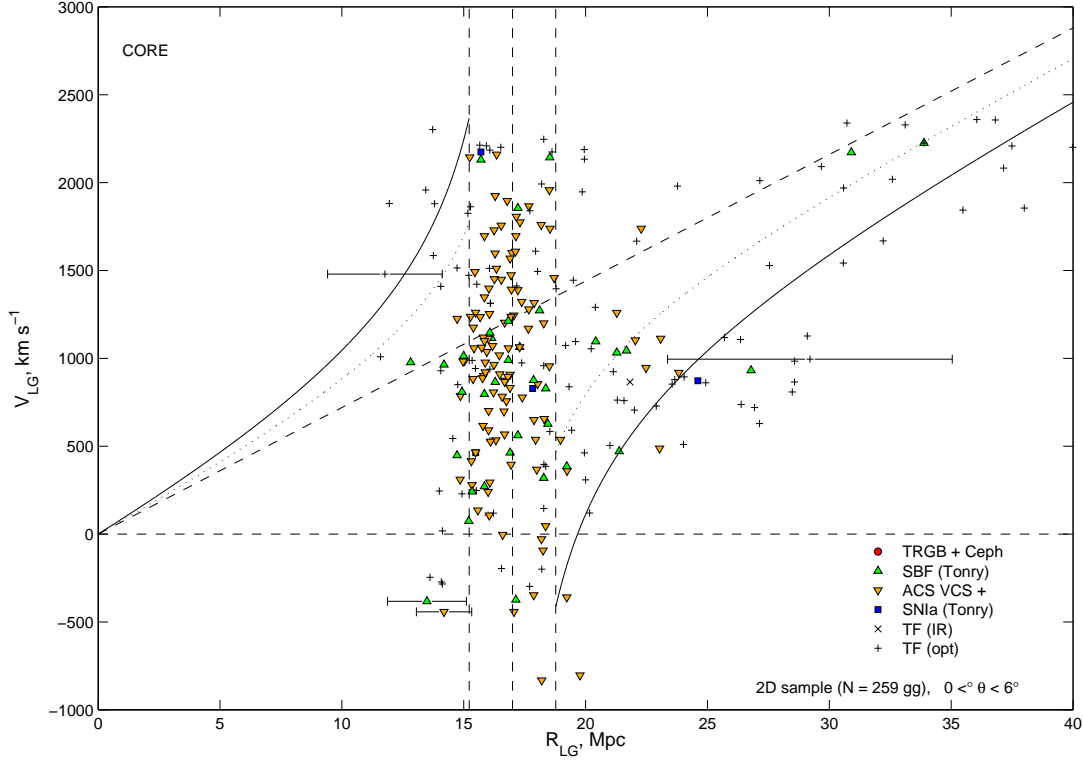


Fig. 1.— The radial velocity vs. distance relation for galaxies in the Virgo cluster region with respect to the Local Group centroid, as shown in Fig. 1 by Karachentsev & Nasonova (2010). Galaxy samples with distances derived by different methods are marked by different symbols. The inclined line traces the unperturbed Hubble relation with the global Hubble parameter $H_0 = 72 \text{ km s}^{-1} \text{ Mpc}^{-1}$. The vertical dashed lines outline the virial zone. The solid and dotted lines correspond to Hubble flow perturbed by virial masses of 2.7×10^{14} and $8.9 \times 10^{14} M_\odot$ as the limiting cases within the confidence range at $\Theta = 0^\circ$. The typical distance error bars for each dataset are shown.

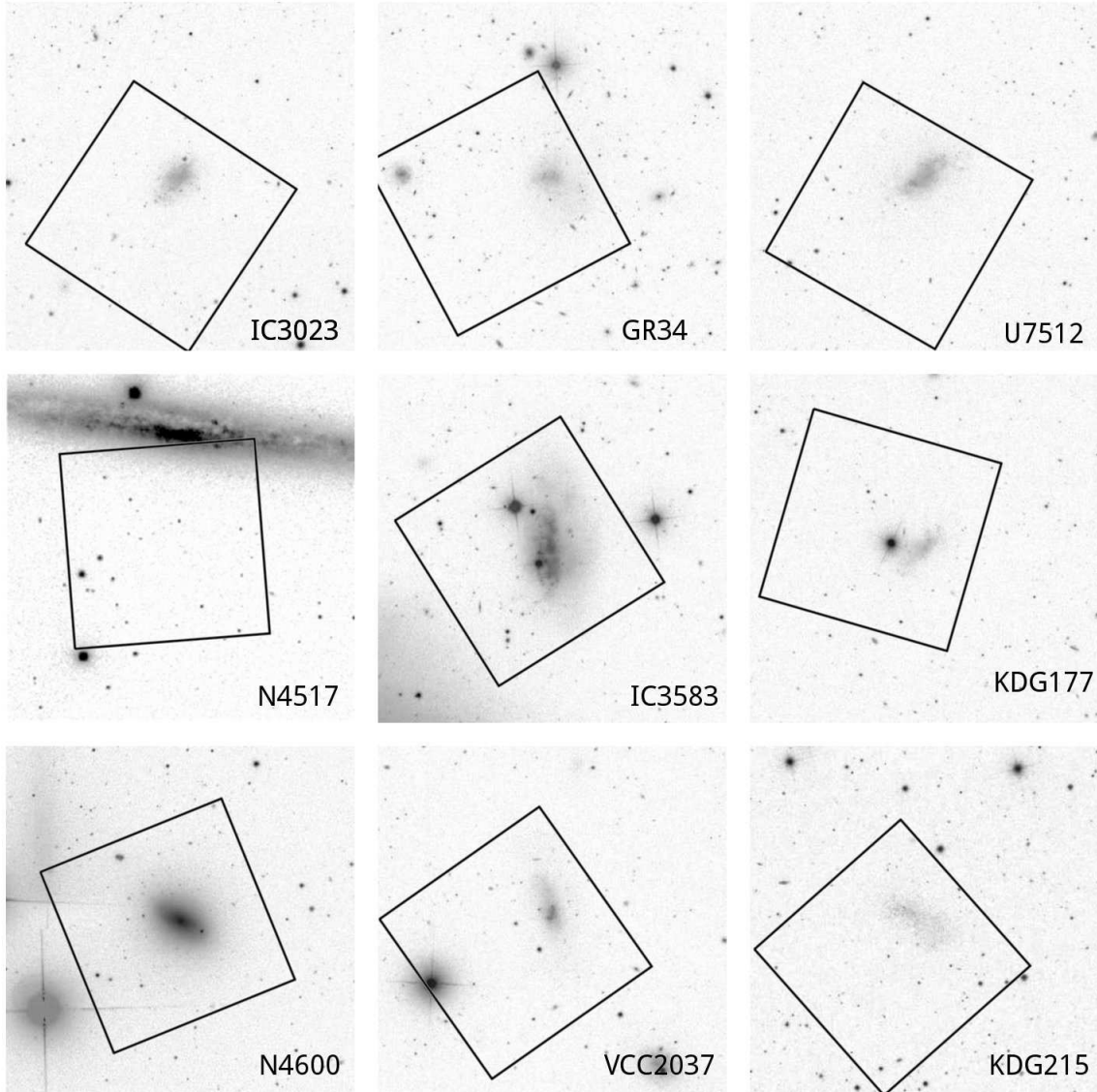
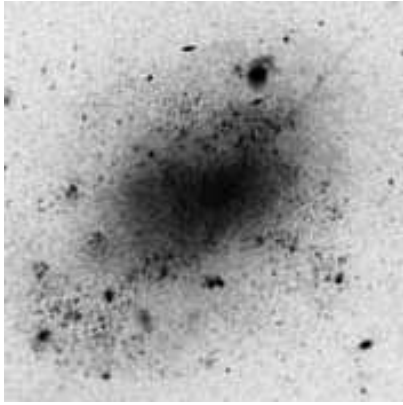
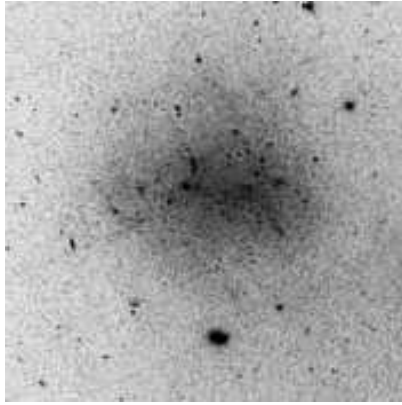


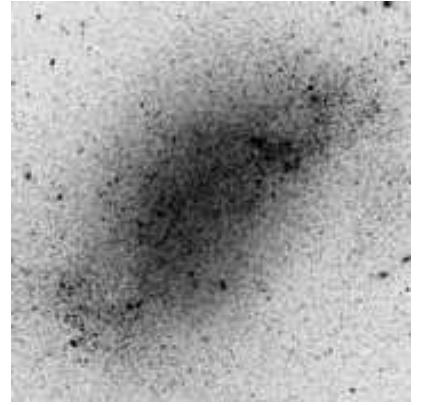
Fig. 2.— Sloan Digital Sky Survey images of nine target galaxies. Each field has a size of 6 by 6 arcminutes. North is up and East is left. The HST ACS footprints are superimposed.



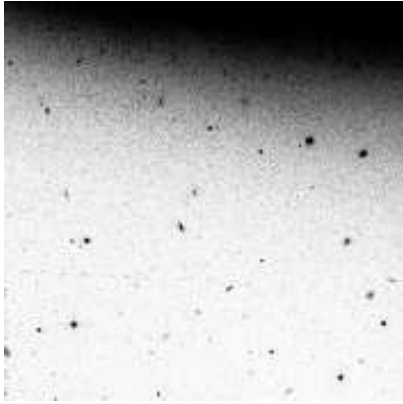
IC3023



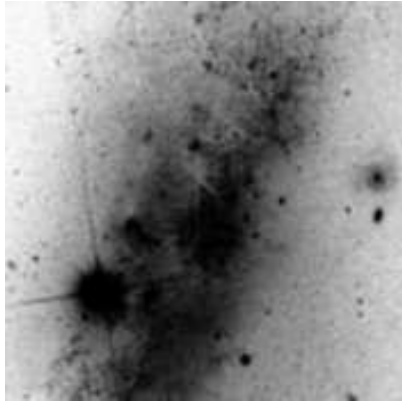
GR34



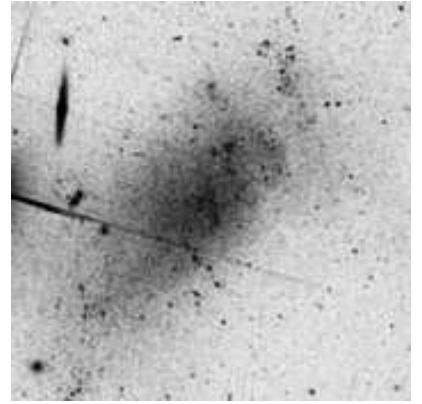
U7512



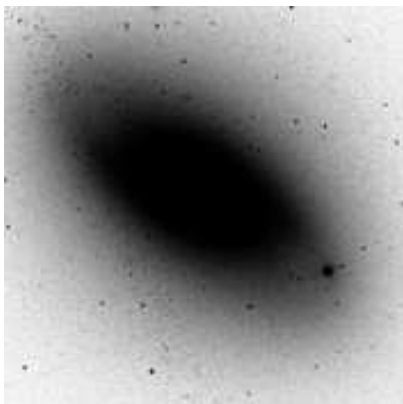
N4517



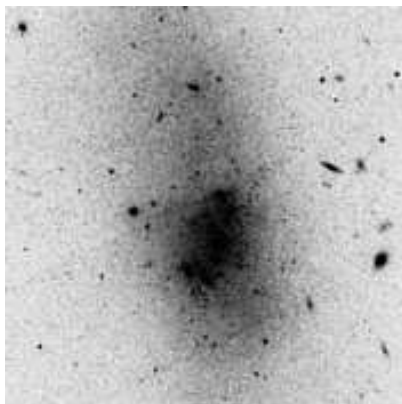
IC3583



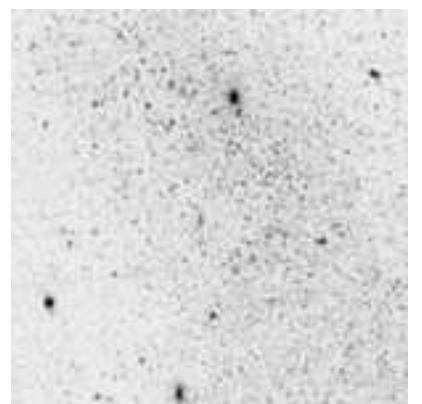
KDG177



N4600



VCC2037



KDG215

Fig. 3.— Mosaic of enlarged ACS (F606W + F814W) images of the nine galaxies. Field sizes are 1 arcminute on a side, North is up and East is left.

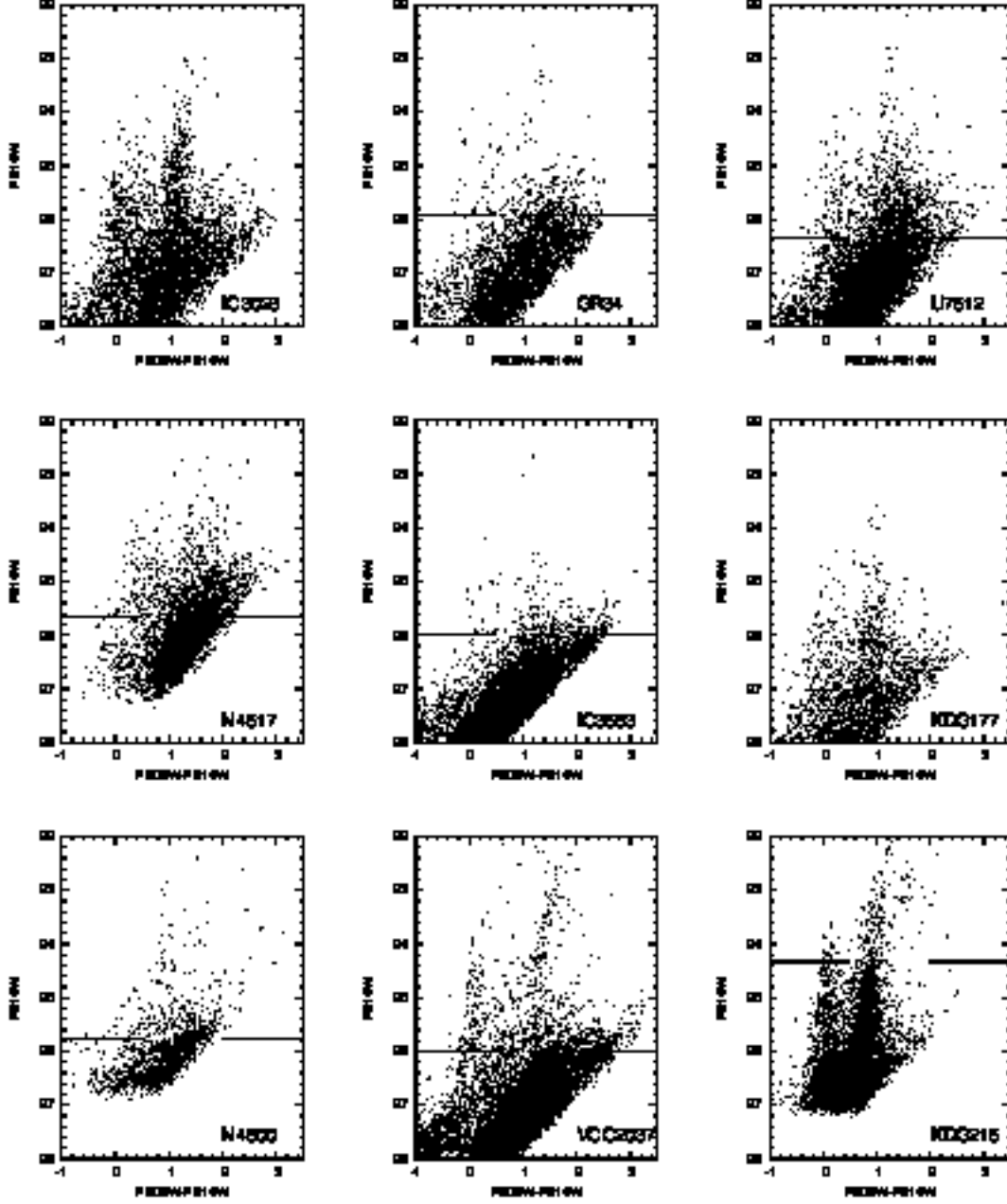


Fig. 4.— Color–magnitude diagrams for nine target galaxies from ACS observations. The broken horizontal lines mark the magnitudes of the TRGB.

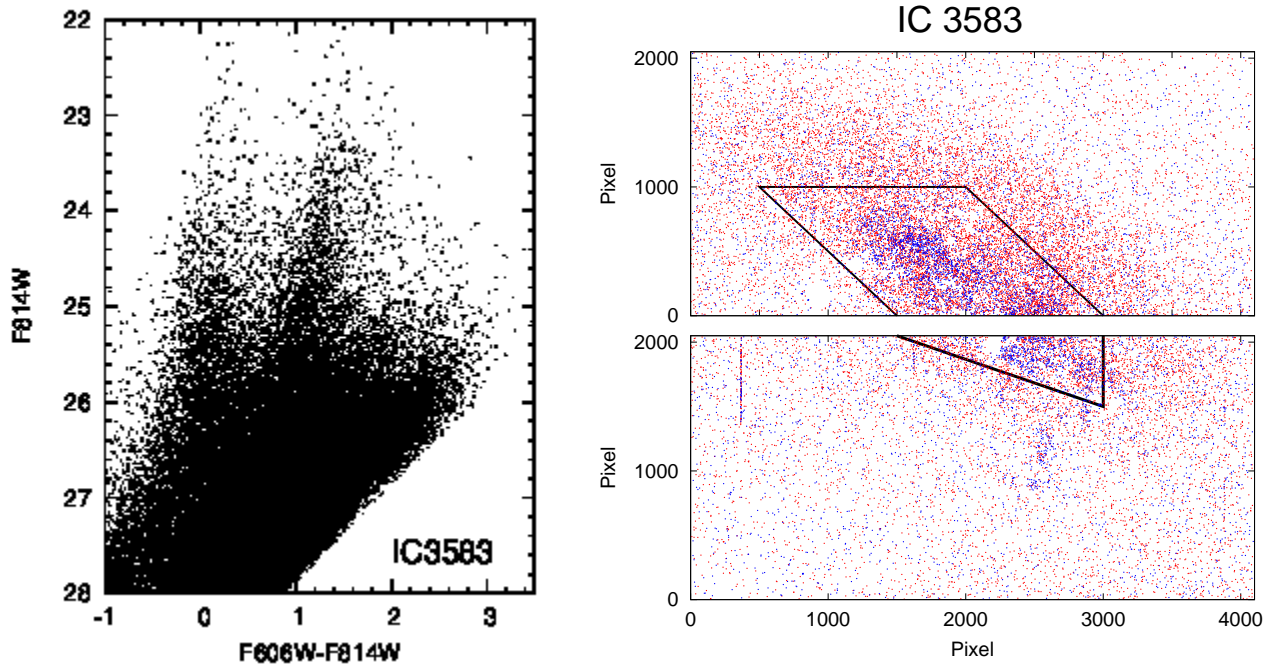


Fig. 5.— Example of spatial clipping to reduce contamination from young populations on the TRGB measurement. The left panel shows the full field CMD for IC3583. The right panel gives the positions of stars in the ACS field with stars with $F606W-F814W > 0.6$ in red and stars with $F606W-F814W < 0.6$ in blue. Blue stars are concentrated toward the center. Only stars outside the exclusion box are included in the CMD for this galaxy shown in Fig. 4.

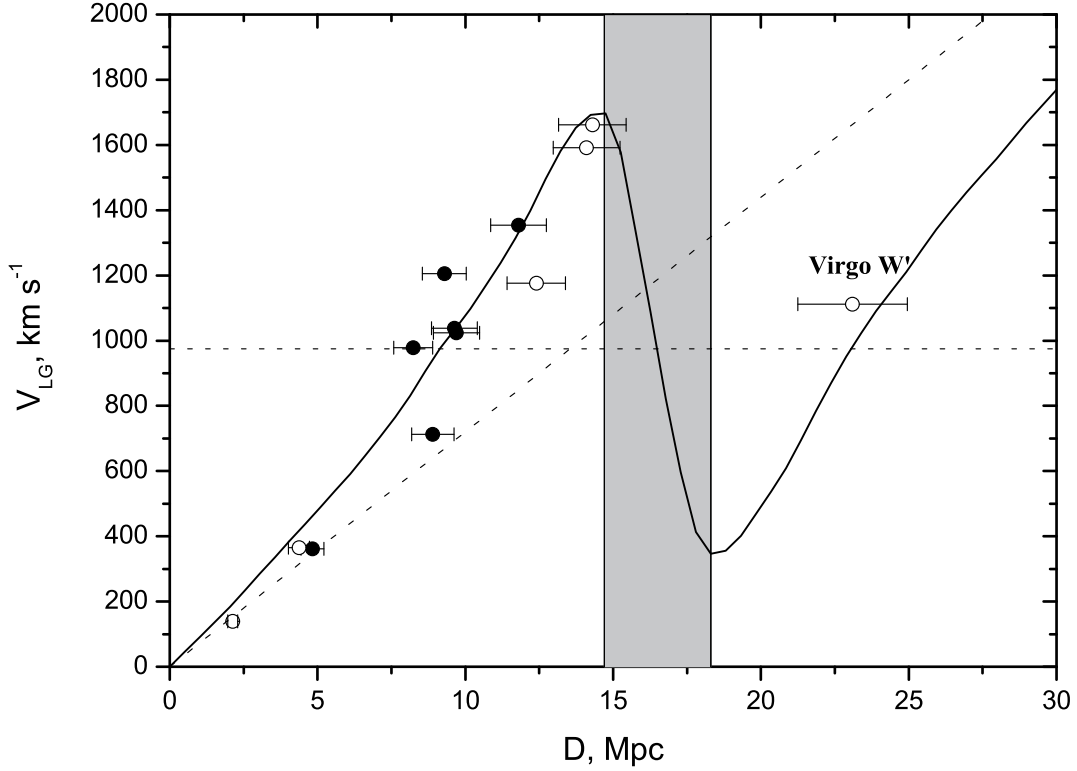


Fig. 6.— Hubble flow in front of the Virgo cluster. Filled symbols: galaxies with new TRGB distance measures from HST observations (Table 1). Open symbols: galaxies with distances drawn from the literature (Table 2). The horizontal bars indicate distance errors. The inclined dashed line marks the unperturbed Hubble flow. The horizontal dashed line corresponds to the mean radial velocity of the Virgo cluster. The grey vertical column denotes the zone of virial motions.